High Voltage Measuring Circuits in AC/DC converters for E-beam Welding Machines.

by

RWAMURANGWA Evode

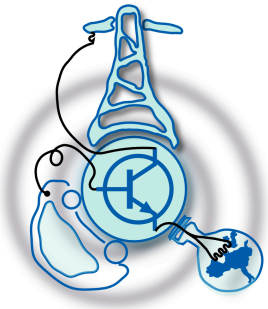

Submitted to the Department of Electrical Engineering, Electronics, Computers and Systems
in partial fulfillment of the requirements for the degree of

Master of Engineering in Electrical Energy Conversion and Power Systems

at the

UNIVERSIDAD DE OVIEDO

Author .....

High Voltage Measuring Circuits in AC/DC converters for E-beam Welding Machines.

by

RWAMURANGWA Evode

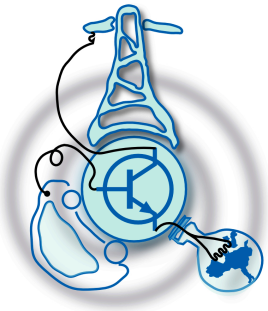

Submitted to the Department of Electrical Engineering, Electronics, Computers and Systems
in partial fulfillment of the requirements for the degree of

Master of Engineering in Electrical Energy Conversion and Power Systems

at the

UNIVERSIDAD DE OVIEDO

July 2015

Author .....

Certified by .....
Juan Diaz Gonzalez
Associate Professor
Thesis Supervisor

High Voltage Measuring Circuits in AC/DC converters for E-beam Welding Machines.

by

RWAMURANGWA Evode

Submitted to the Department of Electrical Engineering, Electronics, Computers and Systems
on July 22, 2015, in partial fulfillment of the
requirements for the degree of
Master of Engineering in Electrical Energy Conversion and Power Systems

Abstract

The Masters Thesis report in case illustrates the design of the High voltage DC (HVDC) measuring circuit. The HVDC will be generated from the Low Voltage DC source using a Parallel resonant converter (PRC); for the intention of supplying a High Voltage E-beam welding machine. First of all the review of the principles of the E-beam welding machine will be re-taken in this work. The same way, the basic principles for the design of the PRC will be illustrated. The full bridge converter based on power MOSFET switches will be built, the adequate firing signals will be generated and strengthened by the drivers; which also will be designed in this work. The control circuit will be designed to give the firing signal; will provide as well the arbitrarity to change the switching frequency and the duty for the purpose of avoiding switching losses and increasing the power transfer to the load. Due, increasing the voltage at the output and managing the power transfer. The expected switching frequency is between $100kHz$ and $150kHz$; while the maximum expected voltage is $3.5kV_{DC}$. The measuring circuit will be made after discussing different ways and choose the best performing. The best isolation system will be made for assuring the security and safety of users. The results at each step will be discussed, conclusions will be made and finally the future work will be suggested.

Thesis Supervisor: Juan Diaz Gonzalez
Title: Associate Professor

Acknowledgments

While finishing this work, I would like to acknowledge the capital support of the Government of Rwanda, It is of big price to heritage knowledge. I would acknowledge the instantaneous support, help, understanding, teachings, patience and advices of **Juan Diaz Gonzalez**; he is more than a professor. I would acknowledge the love care support in everything, from my Parents, My fiancee **UMUGWANEZA Sandra Ghislaine**, all members of my family and friends. you have been every thing for me.

Contents

List of Figures

List of Tables

Chapter 1

General Introduction

The earlier 20th century, was characterized by many trials and development of many new industrial equipments and devices. With the rapid development of computer, electronic and power electronics technology, new components were developed. For instance, Power MOSFET,IGBT and etcs. The last, gave the power and electronic engineers the arbitrarity to deal with all of different needs. The power electronics development was also the solution to the conflicts between DC and AC power. The building of different types of converters gave a way straight forward to bilateral energy conversion. Different electronic structures were developed depends on the targeted use, and based on the present source of energy and the nature of the system to be supplied. In the earlier of the AC electric power development, it was like know that each component connected to the source has to be working on the grid frequency. With the innovations described above, nowdays it is free and easy to supply the system at a needed frequency. The last was due to the development micro-controller, intergrated circuits and sensors. The lastly stated were the key tool to manage the flow of energy from source to destination and following the designer requirement, supply and the supplied system nature. The sensors were used to exactly know the power parameter to be monitored and give the information to the micro-controller, the last will be holding the whole instruction needed to keep tracking the needed or commanded parameters, due the control is done.

The micro-controller, based on the instruction given, and the received parameters, it will generate the firing signals to enable the power switches. The previous text drop us to the target of this work. The work in case is to develop a system that will supply an E-beam welding machine. It is needed to supply the High voltage DC (HVDC) E-beam welding machine from as a low voltage DC source. Looking at it, with the earlier thoughts of DC systems, it could be looked like an impossible thing; but actually it was only matter of time and thinking, then design and implement. Due to the development described before, new components and advanced technology have been successfully applied in E-beam welder as well as the design and manufacture of high voltage have been improved, for instance the use of closed loop control, the high voltage could be controlled automatically, the system quality can be significantly improved. Meanwhile, the application of electronic has contributed to the development of electron beam welder.

During this work, the E-beam welder will be supplied from a low voltage DC source; it is impliedly known that the E-beam works on HVDC source; due, this work will be for providing the electric energy conversion system to supply the E-beam from a low voltage DC source. The Parallel resonant converter (PRC) system will be built working in the range of frequency from 100 kHz to 150 kHz, and with the DC voltage source from $100V_{dc}$ to $200V_{dc}$. The PRC is supplied by a fully controlled bridge rectifier, made of power MOSFET. Due, the last to work; the drivers will be build to strengthen the switching signals from the micro-controller. So, we will build four drivers, one for each power switch. Then we will have the arbitrarity to choose the required wave-forms at the output of the inverter, and it will be voltage in terms. The shape will be discussed in the chapters ahead.

Afterwards, the PRC circuit is added, the last will be made of capacitor for eliminating DC component in the voltage wave-form, the inductor and another capacitor (connected in parallel to make the PRC, at the end will be the parasitic capacitor of the transformer), and the transformer, to step-up the AC voltage to a targeted value.

Then out of the step-up transformer we will have an uncontrolled full-wave bridge rectifier, and a capacitor for filtering, then the required DC output voltage. The last will need to be measured by as circuit design during this work, and the results will be transmitted through an optical Isolating media. The whole system as it will be build is shown in the block diagram in the figure.(1-1). The details for the different

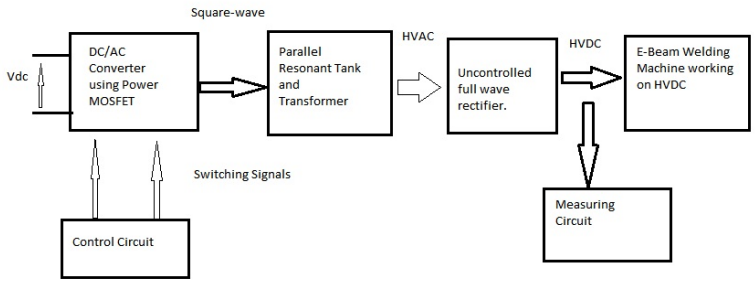

Figure 1-1: Block diagram of the entire model

calculations and designs will be shown in chapters ahead,the results will be discussed, and conclusions will be made and finally the future work will be suggested.

Chapter 2

E-Beam Welding Machine Review

2.1 EBW Description and Principles

The Electron Beam Welding(EBW) is a phenomana that was put into practice after many studies in different laboratories. The EBW is looked as fundamentally unique way to to deliver large amounts of concentrated thermal energy to materials[9].It has been showing great beneficial discoveries and uses industrially . The fundamentals of EBW are easily understood, while being familiar with the main components of the system. The researches shows the main and most common EBW in manufacturing use today to be the high vacuum design (5x10e-4 torr)[9].There are also other type of machines used; those are partial vacuum and non-vacuum equipments. They are typically used in mass production to cop with high output needy. The fig., illustrates important parts of EBM. It generally consists of *Cathode(Filament)*,*Bias Cup(Grid)* and *Anode*. And some sub-assembly components that contribute to the EBW are: High Voltage Insulator Feed-through, High Voltage Cable and focusing and deflection coils. The vacuum vessel is used to house these components;in other words it is called the upper column. The column assembly is held under high vacuum by an isolation valve positioned below the anode assembly.

The beam formation begins with the emission of electrons from the incandescently heated tungsten filament. During this process the filament is saturated by a predetermined amount of electrical current. Electrons boils of the filament tip as it reaches

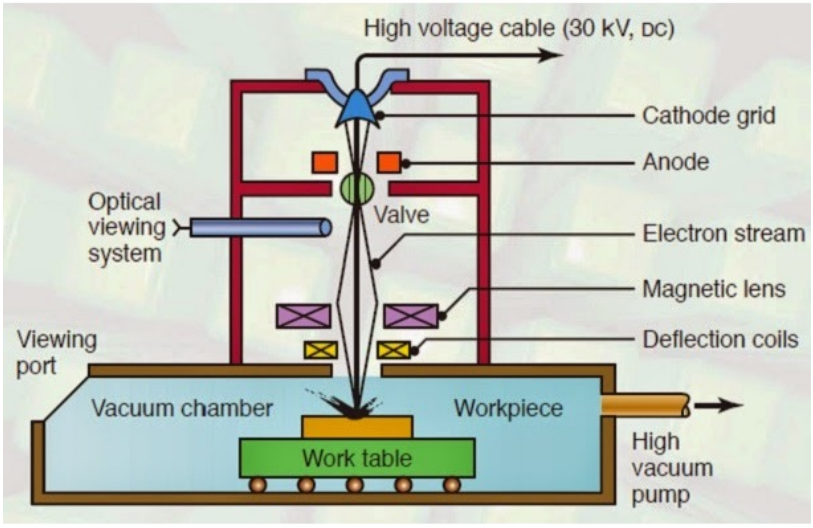

Figure 2-1: Illustration of the EBW process[6]

the operating temperature and gather in the grid cup assembly. A negative high voltage potential is applied to the filament cathode assembly, referred to as the accelerating voltage(kV). With the cathode assembly charged at 150kV[9] the only force preventing the electron beam from propagating is the secondary negatively charged voltage that resides on the grid cup or bias assembly. The voltage in case is lower than the accelerating voltage, acts as a valve that controls the volume of electron energy that can flow from cathode emitter to its attracting target. The anode at a positive potential is one of the attracting targets in the EBW, but its role is more of the beam formation device rather than a collector of electrons. The secondary target is the workpierce which is usually metallic and offers a conductive path to earth to complete the circuit. The electrons gun assembly design is a result of the many extensive engineering studies as well as experimentations. Some of the early EBW design are results of the mathematical model and are still produced.

2.1.1 Beam Delivery

The other components to be taken into account as far as EBW is concerned; to deliver the beam, are the focus and deflection coils and isolation valve. The magnetic coil, located beneath the anode assembly, provides the means for squeezing the beam into

a tightly focused stream of energy or can be used to widely dispersed energy resource. The deflection coil is another very important component that will contribute to the latter discussion of the beam control parameters but for now we will simply say that it is a steering device. The focus coil is circular in design and is concentric with the column. An electric current is passed through the coil which produces the resultant magnetic fluxes that acts to converge the electron beam. Depth to width ratios of (8:1)[9] or greater are achievable depending on the parameters and material conduction. This combination of narrow welds and minimal heat affected zones produced in a vacuum environment results in welds of the highest quality.The deflection coil is configured with four separately wound coils positioned at right angles to the column. The four coils are segmented as sets (x and Y)[9] each axis becomes a separate control allowing the energizing of each axis on command, thus steering the beam. Many industrial applications require the practice manipulation of the beam energy so as to provide a pattern for processing. This is usually accomplished by superimposing an AC signal onto the four coils simultaneously therefore creating a specific pattern. The isolation valve serves to isolate the vacuum environment in the upper column from the lower. After the electron beam has passed through the lower column, it enters the chamber cavity. The last is referred to as an important component that is an integral part of the lower column. In the last, the viewing optics are arranged in such a way that when viewing the beam energy through a video camera or magnified optics it gives the view from a parallel plane, giving the viewer the perception of looking down the column.

2.1.2 Beam Interaction in Chamber Cavity

At the entering of the beam to the cavity chamber, it is targeted onto the material placed at a predetermined height representative of the actual workpiece. This procedure is typical in most pre-weld set-up requirements. The welding technician would then follow a process of beam alignment and beam parameter calibration. Unlike laser, the preparation is quite different in the fact that the technician must view the actual beam through the optical system in order to verify the beam alignment

and focus. With a laser beam, the technician could not view the beam quality and therefore must rely on instrumentation to profile the beam energy. Once the beam has been tuned and calibrated,the equipment is now ready for part processing. The electron beam weld technician is typically a high skilled individual that has a number of responsibilities, there are several skills that the technician must possess in order to ensure safe operation of the device.

2.1.3 Electron Beam Interaction in Materials

The focused beam of electrons is directed at a targeted location on the weld joint at which point the kinetic energy of the electrons is converted to thermal energy. The workpiece can either be stationary and the beam energy deflected or the workpiece can be traversed along a desired axis of motion. This motion can be computer controlled. As the beam energy is applied to the moving part several physical transformations take place. The material instantaneously begins to melt at the surface, and then a rapid vaporization occurs followed by the resultant coalescence[9]. Two welding modes can be used, those are *Conductance mode or a Keyhole mode.*. The conductance mode, primarily applicable to thin materials, heating of the weld joint to melting temperature is rapidly generated at or below the materials surface followed by the thermal conductance throughout the joint for complete or partial penetration. The resultant weld is very narrow for two reasons; first it is produced by a focused beam spot with energy densities concentrated into a 0.010" to 0.30" area[9]. Secondly, the high energy density allows for rapid travel speeds allowing the weld to occur so fast that the adjacent base material does not absorb the excess heat therefore giving the EBW process its distinct minimal heat affected zone. The *Keyhole* mode is used when deep penetration is a requirement. This is possible since the concentrated energy and velocity of the electrons of the focused beam are capable of subsurface penetration. The sub-surface penetration causes the rapid vaporization of the material thus causing a hole to be drilled through the material. In the whole cavity the rapid vaporization and sputtering causes a pressure to develop thereby suspending the liquidus material against the cavity walls. As the hole is advanced along the weld joint by motion of the

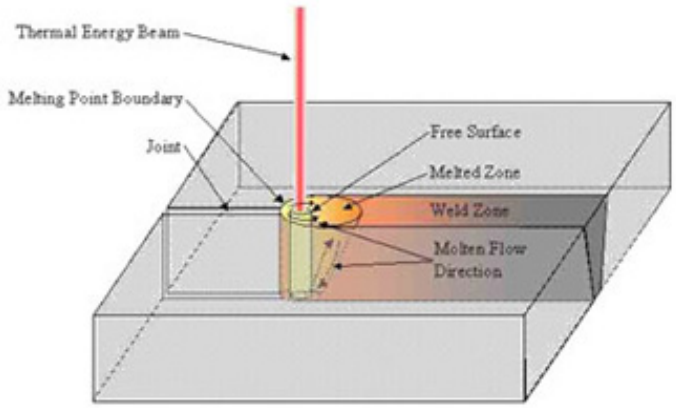

Figure 2-2: Illustration of targeted material[9]

workpiece the molten layer flows around the beam energy to fill the whole welding and coalesce to produce a fusion weld. The hole and trailing solidifying metal resemble the shape of the fashion keyhole. Both the conductance and keywhole welding modes share phyiscal features such as narrow welds and minimal heat affected zone. The basic difference is that a keyhole weld is full penetration weld and a conductance is usually carries a molten puddle and penetrates by virtue of conduction of the thermal energy.

2.1.4 EBW Power Supply

As it was described previously, for the EBW to work, it has to be supplied with an electrical system. This subsection will give an overview on the system that is used to supply electricity to it. The EBW have to be provided with an appropriate power supply for the beam generator. The accelerating voltage may be chosen between 30 to 200kV[10]. Usually it is about 60 to 150 kV[10], depending on various conditions. With the rising voltage the technical problems and the price of the equipment rapidily increase, hence, whenever it is possible a lower voltage of about 60kV is to be chosen. The maximum power of the high voltage supply depends on the maximum depth of the weld required. The high-voltage equipment must also supply the low voltage, above 5V, for the cathode heating, and negative voltage up to about 1000V[10] for

control electrode. This chapter was for giving the reader the reason why we need to design a high voltage supply system for E-Beam. And the rest will be discussed in the next chapters.

Chapter 3

Parallel Resonant converter Review

3.1 Introduction

It is predicted to have in the chapters ahead the system designed to supply the EBW discussed previously. This chapter will give the view of the methodology used to achieve the DC high voltage needed. Due to the fact that most of electric installations found in most of the places are AC; and the EBW needs to be supplied by DC high voltage; then the conversion system need to intervene. There are alot of types of converters that can be used; which implies that not all of them can be used for a single work. Then, the choices was made, and this work will take a *Parallel Resonant Converter (PRC).*

3.1.1 Resonant Converters

The PRC is one of the converters in class of resonant converters; whose operation differs significantly from the PWM converters. The resonant power converters contain *resonant L-C* networks whose voltage and current waveforms vary sinusoidally during one or more subintervals of each switching period. DC- to-high-frequency-AC inverter are required in a variety of applications, including electronic ballasts for gas

discharge lamps, induction heating, and electro-surgical generators. These applications typically require generation of a sinusoid of tens or hundreds of kHz, having moderate or low total harmonic distortion. A switching network produces a square wave voltage $V_s(t)$. Whose spectrum contains fundamental plus odd harmonics. This voltage is applied to the input terminals of the resonant converter network. The network resonant frequency f_o, is tuned to the fundamental component of $V_s(t)$, that is to the switching frequency f_s, and the network exhibits negligible response at the harmonics of f_s. Consequently, the network current $i_s(t)$, as well as the load voltage V(t) and the load current i(t), have essentially sinusoidal waveforms of frequency f_s, with negligible harmonics. By changing the switching frequency f_s (close to or further from the resonant frequency f_o, the magnitudes of $i_s(t)$,$v(t)$, and $i(t)$ can be controlled. A variety of *resonant networks* can be used; among them there is *Parallel Resonant Converter*. The last will be detailed in this work. And its design will be made in the chapters ahead.

3.1.2 Parallel Resonant Converter

The parallel resonant DC-DC converter differs from the series resonant converter in two ways. Firstly, the capacitor tank appears in parallel with the rectifier network rather than in series: due the transfer function $H(s)$ to have a different form. Secondly, the rectifier drives an inductive-input low-pass filter. Consequently, the value of the effective resistance R_e differs from that of the rectifier with a capacitive filter. In order to understand the operation of the parallel resonant converter, sinusoidal approximations can be used. In the Parallel resonant converter, the output rectifier are driven by the nearly sinusoidal tank capacitor voltage $V_R(t)$, and the diode rectifiers switch when $V_R(t)$ passes through zero. If the filter inductor current ripple is small, then in steady-state the filter inductor current is essentially equal to the dc load current I. The rectifier input current $i_R(t)$ is therefore a square wave of amplitude I, and is in phase with the tank capacitor voltage $V_R(t)$. The PRC can be modeled as follows in the figure. 3-1. As it was previously stated, the PRC will be operated at high voltages, it will be necessary to keep an adequate distance between

coils which lead to high leackage inductance L_s[4]; this is due to insulation issues. So, a secondary parasitic capacitor enough to be ignored appears (C_p)[4]; it is due to high transformer ratios, which requires a large number of turns at the secondary. The parasitic elements so generated will be later used to filter the square wave that we shall generate. Due, L_s, C_s and C_p will have a sinusoidal wave form. In order to perform the system calculations and avoid complications, the first harmonic approach will serve better. Considering that C_p and L_s are parts of the transformer, it will

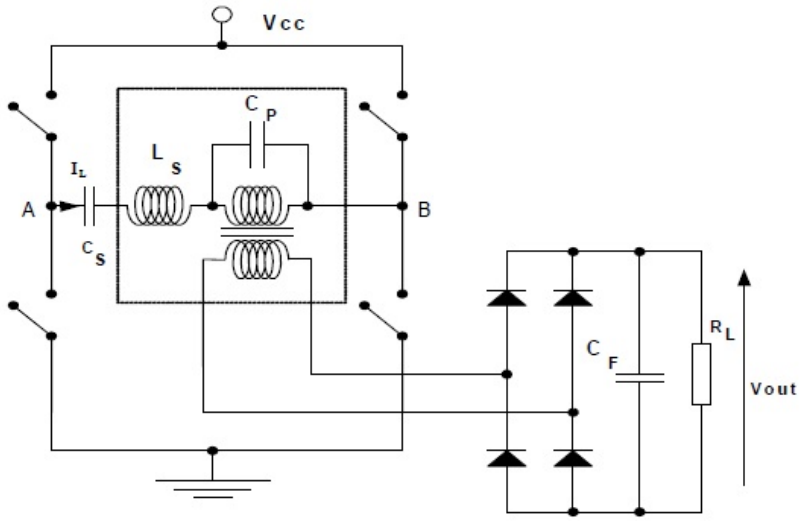

Figure 3-1: The model of the PRC including all the parasitic component of the Step up transformer[4]

.

be an advantage to decrease the number of components needed in the system, and a good economical solution. Due, the transformer has been idealized, for facilitating calculations and the model in figure. (3-2) was used, with $L = L_s$. The wave-forms

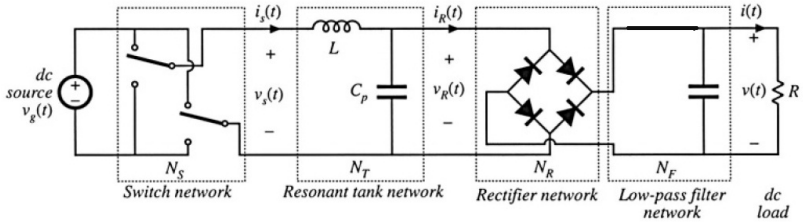

Figure 3-2: PRC block diagram[5]

similar to the ones we will be having in figure.(4-6) will drive the PRC, and the serial

capacitor C_s to block the DC component as it will be detailed later.

Converter Analysis

The converter analysis will be carried out in different stages, as the transformer was idealized and neglected, the process is now simplified, we are only remaining with the resonant tank. If we have a look at the voltage wave-form, the parallel capacitor , it can be noted that the voltage is clamped to the output voltage (positive or negative), when it reaches this value [4]. Based on the *Clamping Time*; we can distinguish two modes of operation, like shown in figure. (4-6). Considering the base values in the equations .(3.1)

$$V_B = V_{cc}, Z_B = \sqrt{\frac{L_s}{C_p}}, \omega_B = \frac{1}{\sqrt{L_S C_p}}[4] \tag{3.1}$$

Mode I

The output voltage is at this case assumed to be constant during the full wave switching period T[4], taking into account the figure.(4-6). Once the parallel capacitor reaches the output voltage level V_{out}, it will no longer charge, since the output filter acts as a voltage source placed in parallel with this capacitor. Once the resonant current falls to zero and becomes negative, the parallel capacitor will begin to discharge, and the current across the diode will be zero, the voltage across the capacitor is clamped, considering that V_{AB} is positive and equal to V_{cc}. Due, the condition in equation.3.2 is defined.

$$t_L >= 0, t_L + t_c <= d.T \tag{3.2}$$

This is a typical high duty-cycle operation mode; as the parallel capacitor has enough time to clamp. This mode will be limited by $t_L = 0$ and $t_L + t_c = dT$. At a fixed duty, a complete system of equations can be got; and it will allow to obtain the different current, voltage and time.

Mode II

In the following mode, $t_L >= 0$ and $t_c + t_L >= dT$; due the parallel capacitor is clamped to output voltage after the input voltage becomes zero. So the limit will be set at $t_c + t_L = 0.5T$, since it is not possible to extend the capacitor voltage beyond this point. This mode appears when the duty cycle is not high, and there is no enough time to charge the parallel capacitor. Depending on the frequency and voltage gain, it is possible to operate the converter with the same duty in both modes, and in both mode soft-switching can be achieved[4].

Optimum Mode

The mode is considered to be optimum, when referring to the case which $t_L = 0$, in this case no reactive power handled and all energy is transferred to the secondary side, this implies the zero current at switching. Due the Zero Voltage Switching is achieved, and a minimum current is needed to charge and discharge the parasitic components of the Power MOSFET[4]. The figure.(3-3) shows the two different modes. In order to

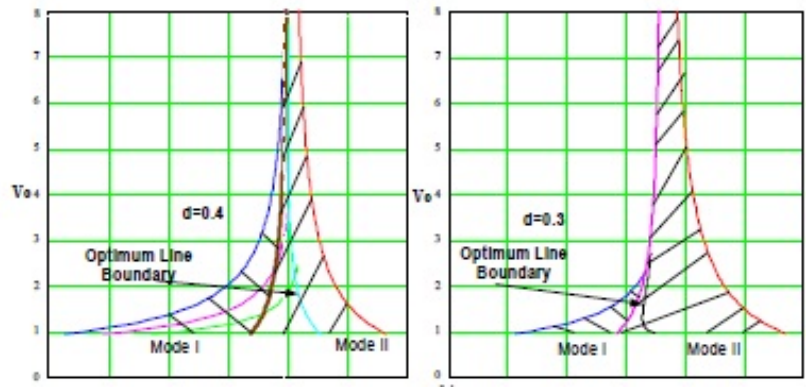

Figure 3-3: Operation mode I an II for two different Duty Cycles[4]

be able to plot different modes of operations and retrieves the required parameters, it the following lines we shall have all of the needed equation and the related equivalent circuits.

System equations and Paramater Calculations

Mode I

In this mode, C_p is clamped before dT, and it corresponds to the optimum mode as we the time lag between current and voltage is zero. Due, the equivalent circuit in figure.(3-4).

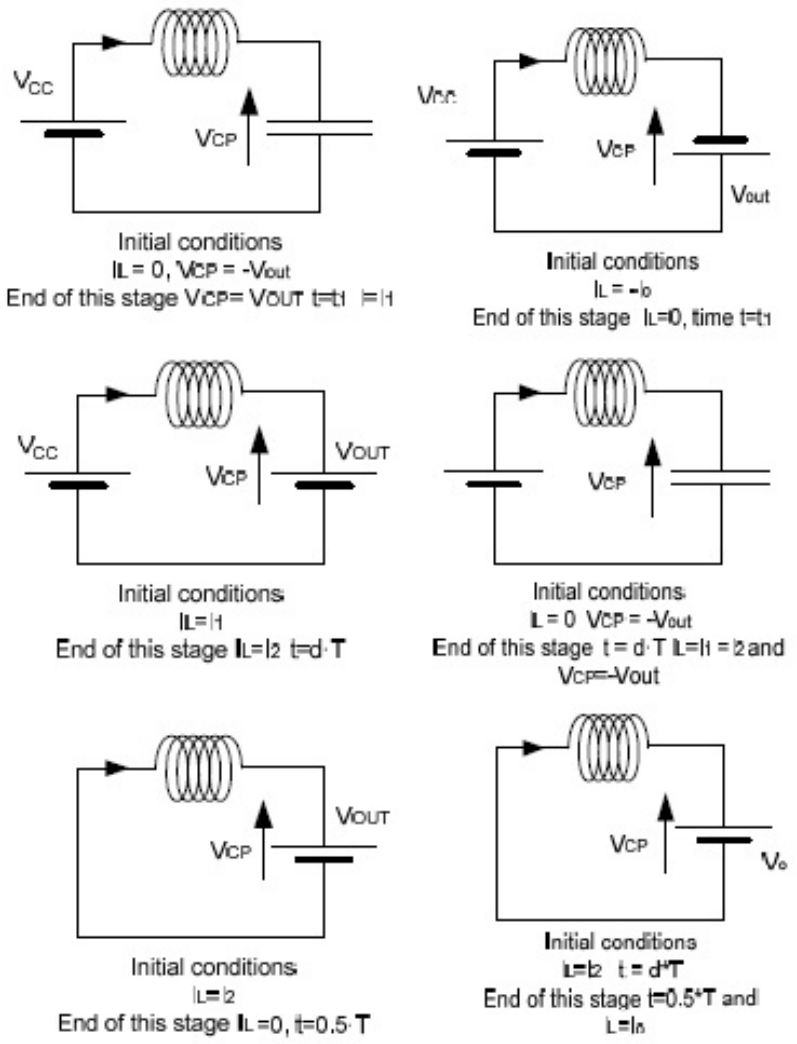

Figure 3-4: Mode I boundery equivalent circuits[4]

The related equations are shown in equation.3.3, corresponding to the left equiv-

alent circuits of the figure3-4. $H = T$ and $h = t$

$$V_o = \frac{(1+V_o)}{2}[1 - \cos(h_1 * 2 * \pi)];$$

$\mathrm{I}_2 = (1 - V_o) * (d * H - d * h_1) * 2 * \pi + 1;$

$H > 0$; $\mathrm{h}_1 <= d * H;$

0=$\mathrm{I}_2 - V_o * (0.5 - d) * H * 2 * \pi;$

$\mathrm{I}_1 = (1 + V_o) * \sin(h1 * 2 * \pi)$(3.3)

The three equivalent circuits corresponding to the right side of the figure3-4 show the boundary between mode I and II, which means C_p is clamped just at $d.T.$ time. Illustrated in the equation. 3.4.

$$h_1 \frac{-I_o}{(1+V_o) * 2 * \pi}; V_o = \frac{(1+V_o)}{2} * [1 - \cos((d * H - h_1) * 2 * \pi)]; I_2 = (1+V_o) * \sin[(d * H - h_1) * 2 * \pi]; -I_o = I_2 - \quad (3.4)$$

Mode II

In this case, the mode II equivalent circuits and equations will be shown. The C_p is clamped after $d * T$; due three different equivalent circuits will be got. And illustrated in the figure 3-5.

It will correspond to the following equations.3.5

$$h_1 = \frac{-I_o}{(1+V_o) * 2 * \pi};$$

$\mathrm{I}_2 = (1 + V_o) * \sin((d * h - h_1) * 2 * \pi);$

-$\mathrm{I}_o = -V_2 \sin((0.5 * H - d * H) * 2 * \pi) + I_2 * \cos((0.5 * H - d * H) * 2 * \pi);$

$$\mathrm{V}_o = V_2[\cos((0.5*H-d*H)*2*\pi)-1]+I_2*\sin((0.5*H-d*H)*2*\pi)+V_2; (3.5)$$

Optimum Mode

At this time, will be defined the optimum mode, in which current and voltage are in phase; and they will be illustrated in figure.(3-6). Corresponding to the following equations.3.6.

$$I_2 = -V_1 \sin[(h_2 - d*H)*2*\pi] + I_1 * \cos[(h_2 - d*H)*2*\pi]$$

$$\mathrm{I}_1 = (1+V_o)*sin(d*H*2*\pi);$$

$$\mathrm{V}_1 + V_o = (1+V_o)*(1-\cos(d*H*2*\pi));$$

$$\mathrm{V}_o = V_1*[\cos(h2-d*H)*\pi-1]+I_1*\sin((h_2-d*H)*2*\pi)+V_1;$$

$$\mathrm{I}_2 = V_o*(0.5*H-h_2)*2*\pi; (3.6)$$

Considering the equation.(3.1), and the specified value of the voltage, frequency, impedance, and expected output voltage; the normalized values can be calculated. With the equations. (3.3),(3.4),(3.5) and (3.6) related to different modes described previously, the different plots can be made. From the figures (3-7) and (3-8), the PRC parameter values can be retrieved. The parameters calculated will be used in the next chapter when design will be concerned.

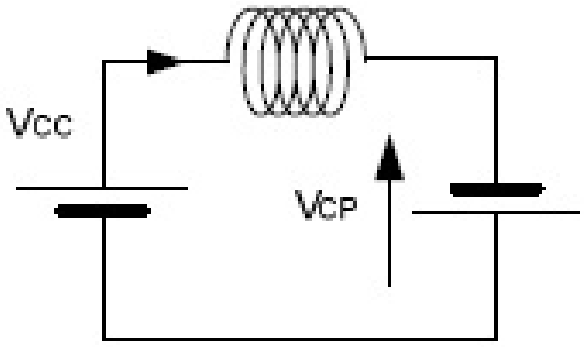

Initial conditions
$I_L = I_0$
End of this stage $I_L = 0$, $t = t_1$ $V_{CP} = -V_{OUT}$

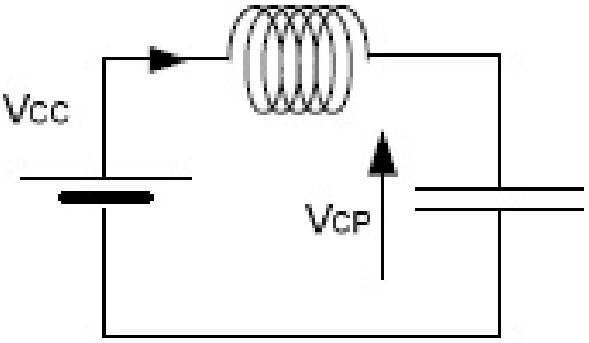

Initial conditions
$I_L=0$, $V_{CP}=-V_{OUT}$
End of this stage $t = d \cdot T$ $V_{CP}=V_2$, $I_L=I_2$

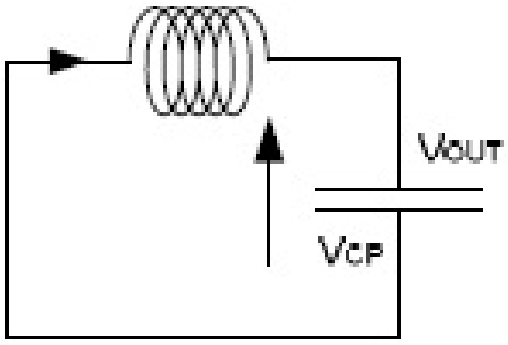

Initial conditions
$I_L=I_2$, $V_{CP}=V_2$
End of this stage $t=0.5 \cdot T$, $I_L=I_0$

Figure 3-5: Boundery in mode II equivalent circuits[4]

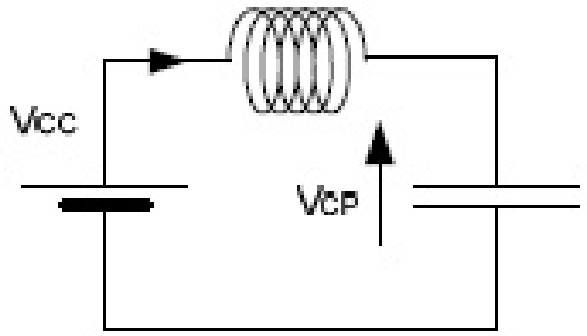

Initial conditions
$I_L = 0$, $V_{CP} = -V_{out}$
End of this stage $V_{CP} = V_1$, $t = d \cdot T$, $I = I_1$

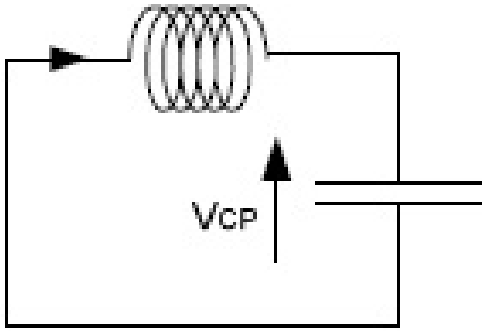

Initial conditions
$I_L = I_1$, $V_{CP} = V_1$
End of this stage $t = t_2$ $V_{CP} = V_{OUT}$, $I_L = I_2$

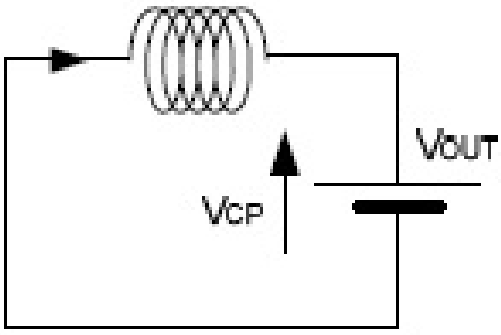

Initial conditions
$I_L = I_2$, $V_{CP} = V_{OUT}$
End of this stage $t = 0.5 \cdot T$, $I_L = 0$

Figure 3-6: Optimum mode equivalent circuit[4]

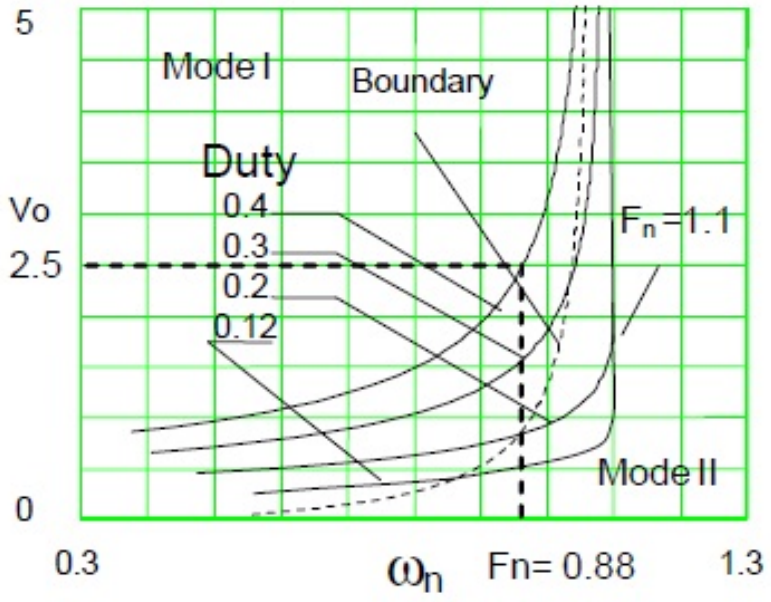

Figure 3-7: Normalized voltage vs Normalized frequency plotted at different values of the duty[4].

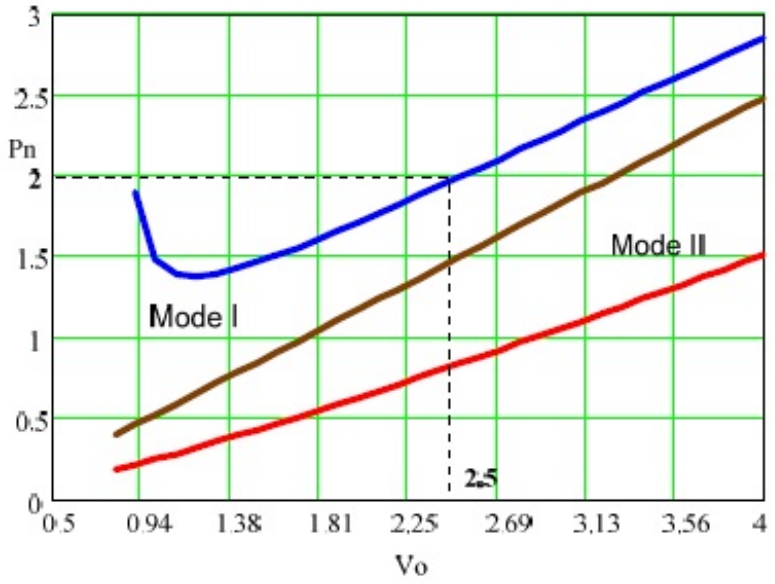

Figure 3-8: Power delivered to the load in all of mode at the value of the duty circle of 0.4[4].

Chapter 4

PRC and Measuring Systems Design

4.1 Introduction

As it was viewed in the previous chapter, the PRC is designed based on the application requirement and other times, based on the will of the designer. Purposely, the designer can make it following his way of choice, based on many hypothesis needed to be proved. Different materials and architecture can be used. Remind back the purpose of this work; it is at the first step to design a converting system, that will be used to supply E-beam welding machine. The second step, will be to design a measuring circuit, that will be used to accurately measuring the voltage supply to the E-beam. As it was showed in the second chapter; the E-beam, in order to work well, it will be supplied by a High voltage DC. In other words; through this work the High Voltage DC enough to function the E-beam will be made, from the Low Voltage DC system. And the measuring circuit will be designed to make sure the DC voltage to E-beam is accurately measured. The conversion system is made of the following important blocks: The DC-AC bridge inverter, the PRC, the step up transformer, and AC-DC diode bridge rectifier as illustrated in figure. (3-1). The next parts of this chapter will give details on the design of each part.

4.2 Converting System Design

The converting system design is made different blocks as it is shown in fig.(3-1) and (3-2); each block has it own design characteristics; the joining of all makes a system.

4.2.1 The DC-AC bridge inverter

This is the two-arms full-wave bridge inverter, connected on the $100-200V_DC$ supply. It is with purpose of converting the supplied DC voltage to the AC voltage. The inverter is made of four $IXFN200N10P$ power MOSFETs; the last ones are the used power switches. The last, the work they must switched at $100-150kHz$ (frequency details in the next section). The switching signal is given by an IC. In order to be given a necessary magnitude and current to drive the switch. In order to be achieved the Driver circuit is designed.

Control Circuit Design

The term control here used refers to the circuit that will be with the purpose of generating switching signals. Depending on the targeted objectives; usually the switching signals for power switches are designed. As the Power switches here present, make a converter with four of them; i.e two-arm converter. The switching patterns are done to ensure the short-circuit avoidance; due no switches of the same arm can be fired simultaneously. In order to achieve that target; the following procedures were done: First the switching logic was simulated using Psim Software, and the switches are named $T1$, $T2$, $T3$ and $T4$, the two first switches in one arm and the two last in the second arm. The switches $T1$ and $T2$ have to be switched by the same signal but inverted for $T2$. The same way, for $T3$ and $T4$. The adequate shift has to be made between the signals go to first arm and those that go to signal second arm. Through that process, the signals were given in the Fig.(4-1) When all of them are added to give the final output signal. It will result in the Fig.(4-2); with at the end will be the shape of the voltage at the converter output. Apart from the simulated values; the practical implementation was made. The **UC3879** IC was used following its appli-

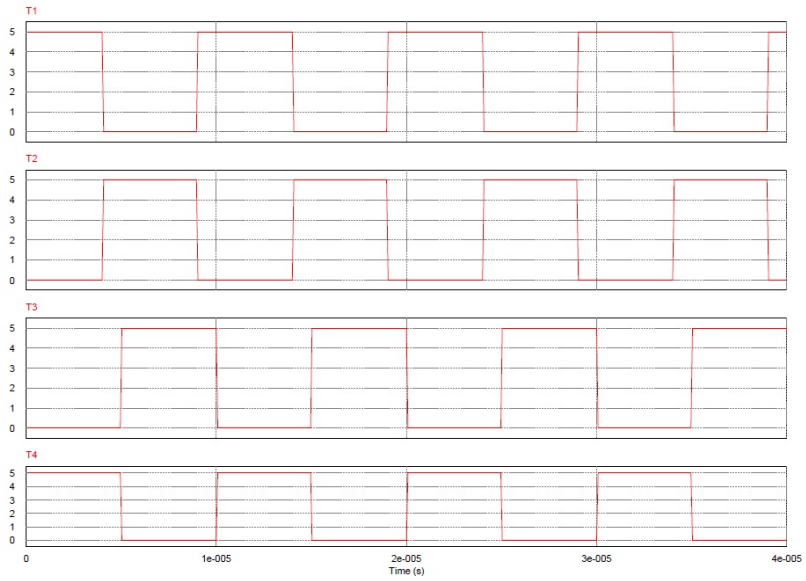

Figure 4-1: Switching Signals

cation note paper[2].The last provides the full information about how to change the frequency as well as the duty and the model was built as it is in the figure.(B-4), the major key to achieve the target was two important parameter, resistor from **RT** pin and Capacitor from **CT** pin. Those two parameters are achieved based on equations. 4.2 and 4.1.

$$RT = \frac{2.5V}{0.01A * D_{osc}} \tag{4.1}$$

and

$$CT = \frac{(1 - D_{osc})}{1.08 * RT * f_{clock}} \tag{4.2}$$

With the chosen frequency, we can manage to have both of the parameters, but the issue was that above the $100kHz$, the value of the capacitor is fixed; and even in normal way, we could not change the capacitor that much to achieve the necessary change. What was done, is to apply the equation.4.1, as it is and give the capacitor a fixed value following the table. A.3. and the system test conditions described in the application notes, we chose the value of $CT = 470pF$ and $RT = 50k$ potentiometer, as it is in the figure.(B-4). Up to this point we could only vary re frequency. The rest was to be able to shift one arm signal in order to be able to create a duty in the final output signal. As the control is done manually, we invented error by connecting

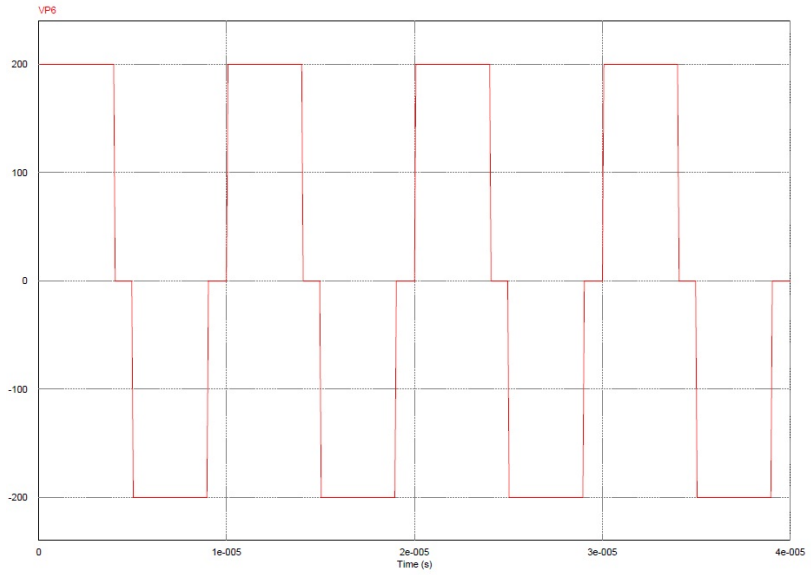

Figure 4-2: Converter output Voltage

a potentiometer at the error amplifier pin **Comp**; which is usually the cause of signal shifts, as it can be seen in figure.(B-4). Due, with the help of the potentiometers we succeeded to change the frequency and the duty of the signals we need. As it will be shown in the schematic (B-4) . The **UC3879** IC, well connected is able to give the four switching signal for the respective four power switches. The Potentiometers on **RT**, **Comp** and **EA** terminals of the IC, help to vary the frequency and well as shifting the signals respectively. Due, they will help in giving that freedom of choosing the switching frequency and a required shifting to achieve the required converter output wave form.

Driver Design

The driving signals are given by the **UC3879** IC at the amplitude of 0-10V, while the needed amplitude to drive the switch is 0-15 V. Due, the driving circuit for each power switch is made.The last is built to give to the switching signal the current necessary to drive the power switches. The circuit in case is made by a **A J312** Opto-coupler[7]. Illustrated by fig.(4-3), the last will produces the adequate signal strength and amplitude to drive the power MOSFETs. It will help also to Isolated the two parts of the driver. The **THL 10-2423WI** DC-DC converter is used to give the necessary voltage

to the opto-coupler. The **MJD45H11(PNP)** and **MJD44H11(NPN)** are at the end connected to amplify the current to the better strength to drive the MOSFETS. The full model for the driver circuit is illustrated in figure (B-6). As the Driver is

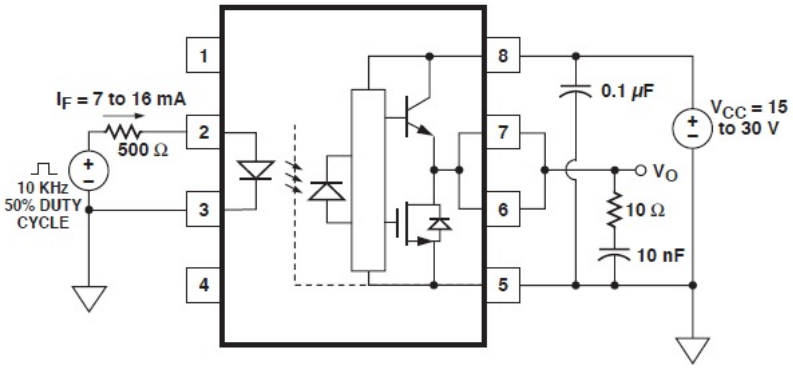

Figure 4-3: Opto-coupler schematic[7].

made and the switching signals are adequately strengthened; the *Bridge inverter* will be switched following the sequence $T1T4$,$T2T4$, $T2T3$ and $T3T1$ which at the end will have to give the signal in fig.(4-4); for voltage and current. The voltage signal still

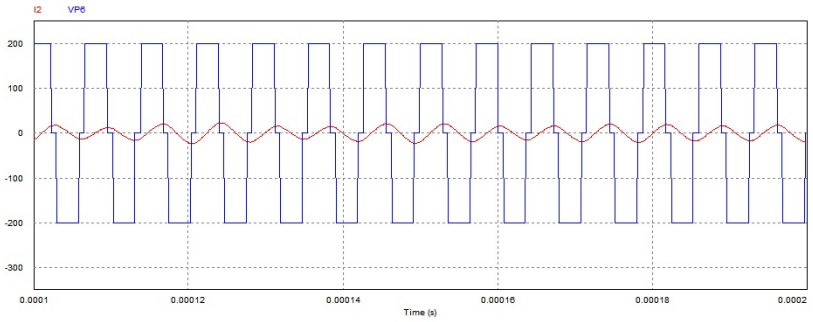

Figure 4-4: I2:Output current, and VP6: Output Voltage

include the DC components, while the objective was to have a smooth AC signal.This case will be discussed in the next lines.

PRC Design

Considering the fig.(3-2), the *PRC* part will be including the all of the components from the bridge inverter upto full bridge diode rectifier. And it will be looking as in

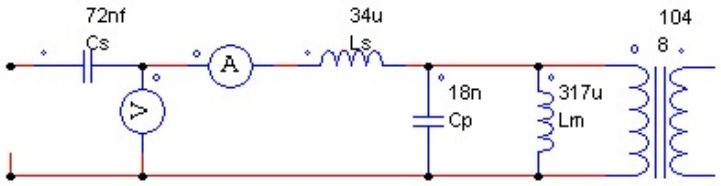

Figure 4-5: PRC model

the fig.(4-5). The capacitor *Cs* will be used for filtering the DC waveform in the square wave-form, thus does not require any special specifications. The components *Cp, Ls and Lm* are intended to be included in the transformer as its parasitic elements; in this case, the number of external components needed is zero unless the transformer parasitic capacitor will not be big enough[4]. As the application in case consists delivering the $3.5kV$ as an output voltage, with the load of $R_L = 47k\Omega$. The input voltage varying from $100V_{DC}$ to $200V_{DC}$. The power delivered will be $260W$. Taking into account the figures (3-7) and (3-8) and the equations (3.3),(3.4),(3.5) and (3.6) togather with the base equations.(3.1), the following values were got and used to simulate the PRC resonant converter. $L_d = 34$, $C_p = 18nF$, $N_p = 8$, $N_s = 104$. After having the last values, the inductor L_d to be used needed to be designed. The design of the inductor was made following the equations below: Considering the length of core air gap $l_g = 1.46mm$, Magnetic Permeability of the free air: $\mu_0 = 4 * \pi * 10^{-7}[Henry/m]$, Section of the core:$A = 9.95mm * 22mm = 218.9mm^2$. Due the Magnetic reluctance of will be shown in the equation. 4.3.

$$R_g = \frac{l_g}{\mu_0 * A} \tag{4.3}$$

And the value will be $R_g = \frac{1.46*10^{-3}}{218.9*10^{-6}*4*\pi*10^{-7}} = 5.3 * 10^6[AT/W_b]$. Taking into account that the magnetic reluctance of the core is negligible compared to that of air. The equation. 4.4 will give us the number of turns need, due to calculations, the

number of turn found was $N = 13$, and it was the one used.

$$L_d = \frac{N^2}{R_g}; N = \sqrt{L_d * R_g} \tag{4.4}$$

Together with others values shown before, they are the ones used in the Psim simulation, as displayed in the figure.(4-5). As the design is done considering the high voltage, the good insulation issue must be taken inti account between the primary and the secondary of the transformer. At the end the single capacitor *Cf* will be used as a filter.

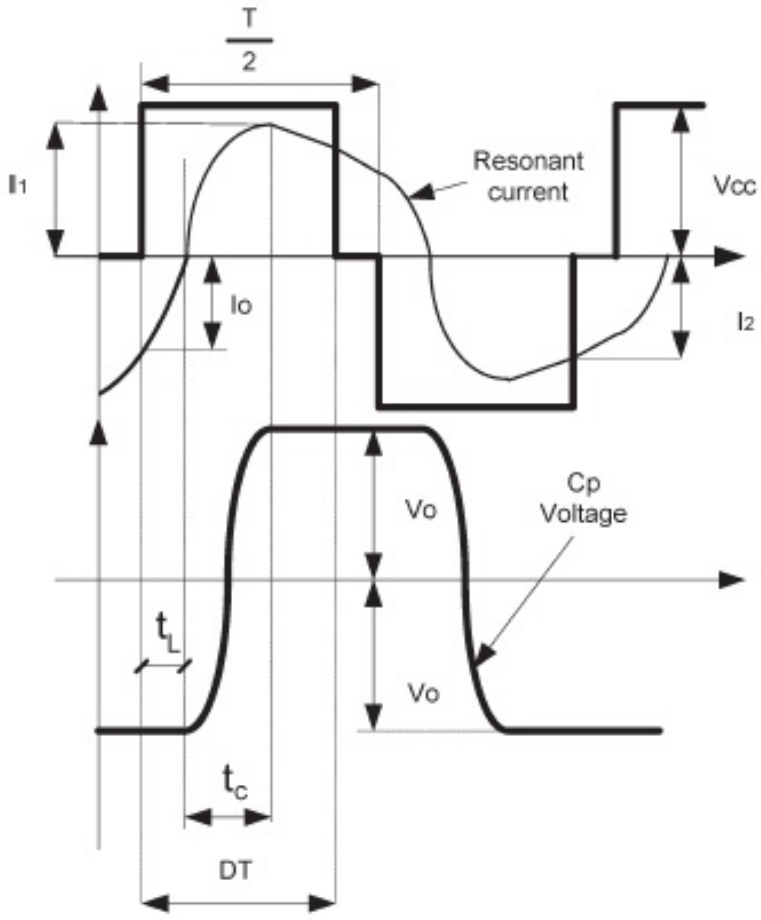

Figure 4-6: Mode I, Square wave-form voltage and resonant current. Mode II Voltage clamp produced after DT[4]

4.3 Measuring Circuit Design

The measurement circuit is referred to as the circuit that will be sensing the value of the generated voltage and outputs a signal of level easily managed. The voltage that is generated by the whole system is $3.5kVDC$. The last one is so big in value to have a measuring instrument. But on the other hand, as that voltage level is needed, it has to be measured for adequate use. The circuit will be designed to interface that big voltage to user quantifier. Due, it will be the measuring instrument. Different methods were discussed in order to achieve a better, easy and accurate way of measuring. This work will consider **Voltage divider Method.**

4.3.1 Voltage divider Method.

The resistive voltage divider, a high voltage can be reduced to weak and low voltage in the range of manageable values. This method presents high precision with measurement error less than 5%. Here, the designer, still is the one who has the last decision, to choose the ratio between the input and the output voltage. It is assumed that the input impedance to the buffer (R_2) is much bigger than R_1,the loading on the divider is negligible. so, the ratio is simply given by the following equation:

$$\frac{V_{in}}{V_{Out}} = \frac{(R_1 + R_2)}{R_1} = 1 + \frac{R_2}{R_1} \tag{4.5}$$

Considering the equation 4.5 and the figure (4-7), having selected norminal values,

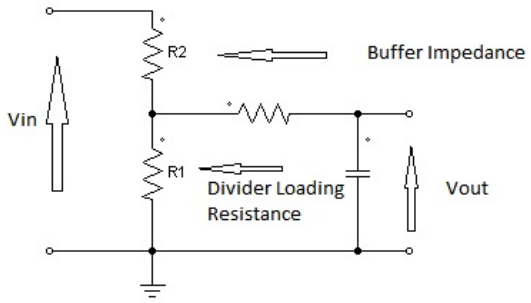

Figure 4-7: Voltage divider

the next consideration will be the tolerance needed. The last one is simply the ratio in the sum of the individual resistance tolerance. It is not mandatory to always have the same tolerance, due and it is mostly more economical to select a tighter tolerance on the low voltage part. It should be noted that the voltage ratio is not the same as the tolerance ratio R_2/R_1 but is offset by one. Due, for a voltage ratio of $1000:1$, it is necessary to define a resistance ratio of $999:1$, here the standard values of resistors have to be chosen. In the case of this work as the design is considered, we decide to reduce the norminal error to 0.001%. Due, the voltage ratio chosen is $10000:1$ and the resistance ratio is 9999. The standard resistances chosen are $R_2 = 10M$ and $R_1 = 1k$ following the table A.2, the value available in the lab were, $R_2 = 8M2+1M8$ and $R_1 = 1K0$. As the full model of this work was simulated in the PSIM software as shown in figure (B-5), the measuring circuit results compared to reals values are also displayed in figure (4-8). Even if this method has an appreciable precision in HVDC measuring, it can analytically presents some predictable problems. Here, it can be shown that the high voltage reference is directly connected to the weak voltage reference; as it is required to display the value of the measured voltage at lowest voltage devices, in case of dangerous high voltage surge for instance during power on, these devices can be burnt easily. The proposed solution to this issue is to use an isolation system.

4.3.2 Isolation Medium

In order to ensure the security of the users as well as the lowest voltage equipments that will be needed on this measuring system, the best isolation has to be used. Many isolation methods were thought, and discussed to find- out the adequate one. The isolation can be made in many ways, but the following were discussed: transformer, opto-coupler and Optic Fibers.

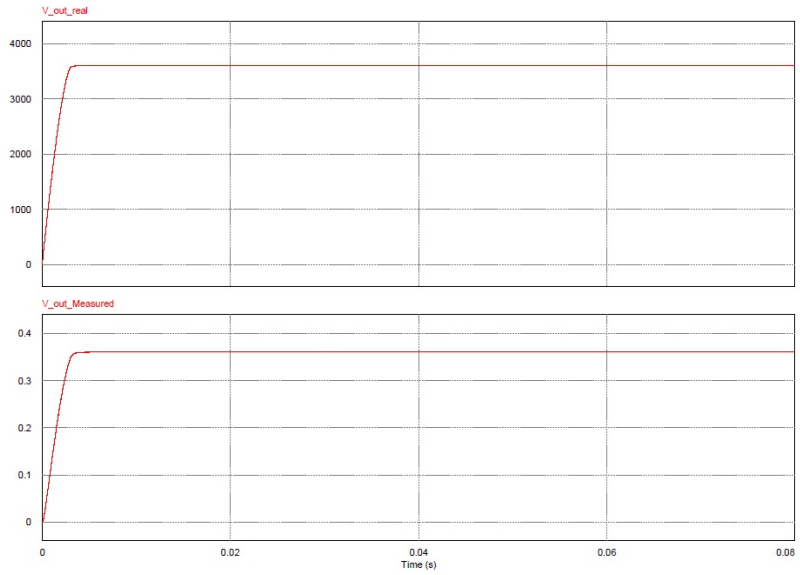

Figure 4-8: Measured and real output voltage value as simulated in PSIM

Transformers

It was suggested to design an inverter to bring back the DC measured value to AC and use a coupling transformer like an isolation tool. The last one in principal should work. unfortunately, it includes many other components, which makes a bigger and heavy as well as expensive system. It should need addition rectifier and inverter, these switching systems in turn need switching modules and biasing voltage sources. all of the previously mentioned drawbacks caused to cancel this method and thinking about a new way.

Opto-couplers

Opto-couplers are semi-conductor based light sensitive devices. It optically links two semi-conductor switches. The last ones present the threshold voltage in order to start conducting. Below the threshold voltage, the semi-conductor switch will not conduct, but once the threshold voltage level is achieved; immediately the semi-conductor switch starts conducting. This characters became a drawback for this research, as we needed to investigate the change in the measured voltage and display the same value at the output. So, in this case, the change below the treshold value can't be displayed

and the changes above treshold value results in a constant output value.

Optic Fibers

It is referred to as a flexible, transparent fiber made by drawing glass (silica) or plastic to a diameter slightly thicker than that of human hair[11]. The Optical fibers are used most often as a means to transmit light between the two ends of the fiber. Due that last property of it, the *Fiber Optic* can be used as an isolator. It will be taking the value at the measuring instrument terminal and transmit it to a display system. This will be a safe way to be accessible by users. They will be completely isolated from the powers circuit. The *Fiber Optic* system is made of the transmitter and receiver; depending on the application, there are different commercial transmitters and receivers.

In case of this work, we chose **HFBR-0500Z Series**, the Versatile Fiber Optic Connection; It is a complete family of fiber optic link components for applications requiring a low cost solution. The **HFBR-0500Z Series** includes transmitters, receivers, connectors and cable specified for easy design.This series of components is ideal for solving problems with voltage isolation or insulation, EMI or RFI immunity or data security. The Optical link design is simplified by the logic compatible receivers and complete specifications for each component. The key optical and electrical parameters of links configured with the **HFBR-0500Z**family are fully guaranteed from 0 to 70'C. A wide variety of package configurations and connectors provide the designer with numerous mechanical solutions to meet application requirements.The optic Fiber System described previously is illustrated in the figure (4-9). The target

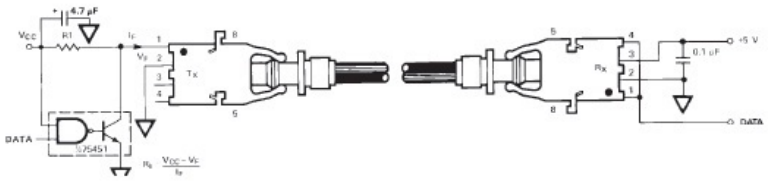

Figure 4-9: Fiber Optic Linkage[8].

was to use this system to isolate the used from the powered system; unfortunately the challange was that, this system was designed for digital signals; It was required to change the DC voltage signal received at the output of the voltage divider circuit into digital form of signal. This required to design another board which will be receiving voltage and gives us a square wave signal at a frequency that will be depending on the input voltage value.

Voltage to Frequency interface

The interface in case was built based on the principles of **XR-2206** Integrated Circuit. The last is a monolithic function generator capable of producing high quality sine, square, triangle, ramp and pulse waveforms of high quality stability and accuracy. The output wave-forms can be both amplitude and frequency modulated by an external voltage over a range of $0.01Hz$ to more than $1MHz$. The circuit is ideally suited for communications, instrumentation and function generator applications. The oscillator frequency can be linearly swept over a 2000 : 1 frequency range with an external control voltage, while remaining low distortion. The *Voltage to frequency interface*

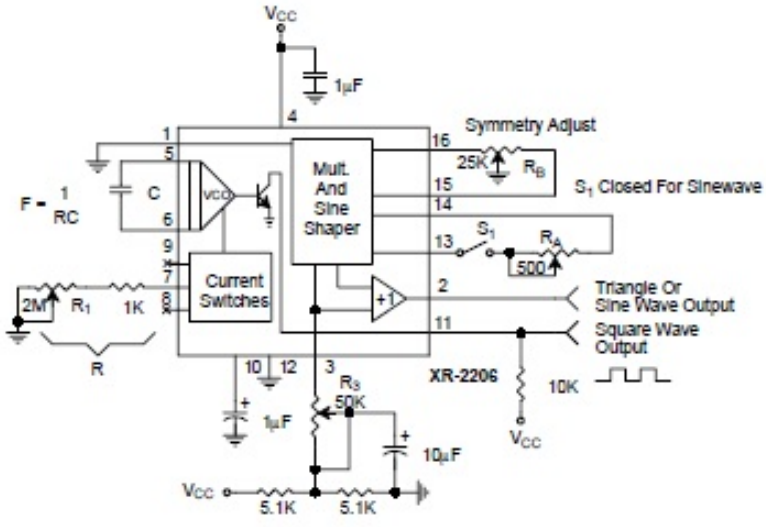

Figure 4-10: Circuit for square wave generation at the required frequency[1].

board was built following the figure (4-10) and at the terminal 7, at which we will need to supply the changes in voltage amplitude, the resistance R is replaced by

the circuit shown in figure (4-11).In which the resistance $R_c = 1k$ and $R = 10k$. The voltage at this terminal seven is always not bigger than $3V_{dc}$, due the maximum value that will be appearing at the measuring device has to be below $3V_{dc}$. This means that the measuring ratio has to be made higher enough to achieve these very small amount of measured values. The input voltage was made $V_{cc} = 12v$ and the capacitor$C = 0.01\mu F$,in the circuit displayed in figure (4-10). From the measuring

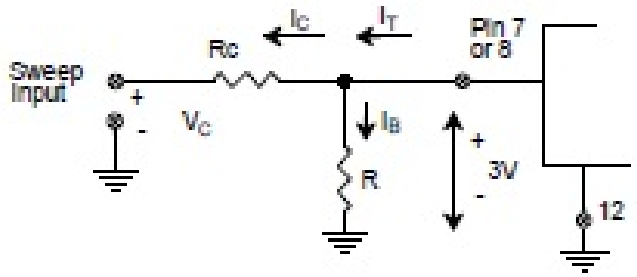

Figure 4-11: Circuit connection for frequency sweep[1].

voltage divider circuit, the measured value is supplied to V_c of the circuit model in figure (4-11) and (B-7). The variation in the measured value, will cause the variation in the value of V_c, due the variation in the frequency of the square-wave measured at terminal 11, as displayed in figure (4-10). Upto this point we will be having the voltage measured converted into frequency. The voltage-frequency relationship is a mostly linear, due we can relate it in the equation (4.6), the equation in case was made based on the measured value of frequency at a step of $0.1v$. from $0.4v$ to $3.0v$, and the results are displayed in the table (A.1).

$$f(v) = -30.814v + 106.05 \tag{4.6}$$

. With $f(v)$: the frequency and v: the measured voltage. Only the frequency here will be the considered parameter, as the signal we have is square in form, it can be transmitted via the fiber optic link. Due, following the link made in figure (4-9), the isolation is made between the user and power circuit. In order to know the value of

the measured voltage, the frequency measured at the output of the fiber optic link with the equation (4.6) will help for calculation, and time the voltage divider circuit ratio, the real value of the voltage will be got. All of these last calculations can be made with a help of a micro-controller, and the measured value can be displayed using a display. Even though this last process was not included in the work up to this step, but it will be in the next steps.

Chapter 5

Results and Discussions

In the previous chapters of this work, different parts of the whole built system were discussed. The method and basic principles used to build the models were shown. Different descriptions and simulations were done. The actual chapter will be showing the practical and real results of the whole system in case.

5.1 Control Circuit results

The control circuit was built, based on the principle discussed previously in the *Control Circuit Design* section. The aim was to verify that the results of the practical models match the one we have got during the simulation in Psim and displayed in Fig.(3.1). After building the prototype as it was required, the results will display the switching signals as follows. Here it can be reminded that, the control circuit has the option to change the frequency as well as the shift of signals between both arms. From the figure (5-1) compared with the figure (3.1), the results are similar; which confirms the conformity of the simulated results with the real prototype results. Due, the switching will be correct too.

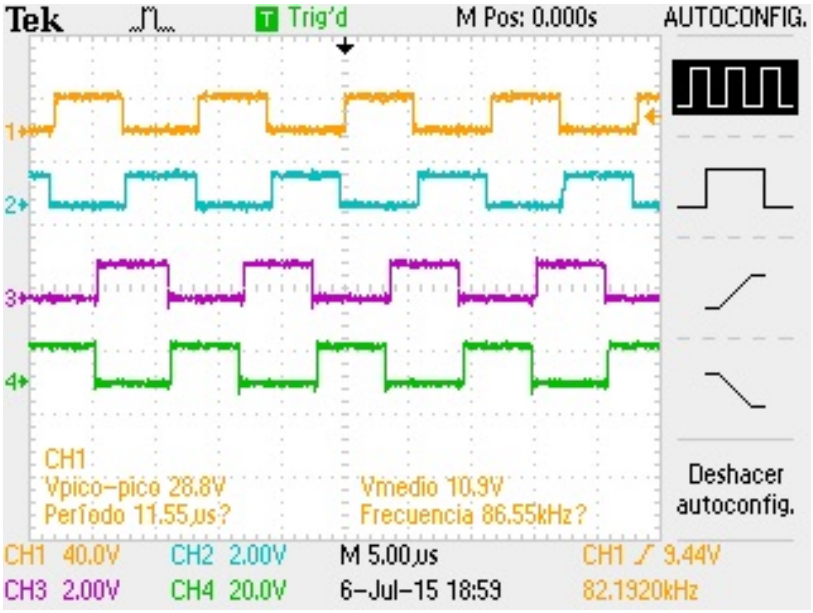

Figure 5-1: The switching signal measured at the output of the control circuit, when the frequency is calibrated to 86.55kHz.

5.2 Driver Results

The drivers were designed as the circuit required to strengthen the switching signals, so that the last can be able to fire the MOSFETs. The design of the drivers were deeply discussed in the previous chapter. This section will only display the results of the switching signal from the control circuit and supplied to the drivers, the output of the drivers have to be the signals similar to the ones got in the Fig.(5-1), with the only difference in amplitude and signal strength i.e the signals have to be of the same shape and frequency. Even it the switching signal from Fig.(5-1) and those from Fig.(B-3) are of the different frequencies; here it can be reminded that the frequency can be changed according to the need of the operator. Both are of the same shape, except that the ones from drivers are strengthened and greater amplitude and current enough to fire the MOSFETs. Due, it can be concluded that the drivers work also as they are required in the design.

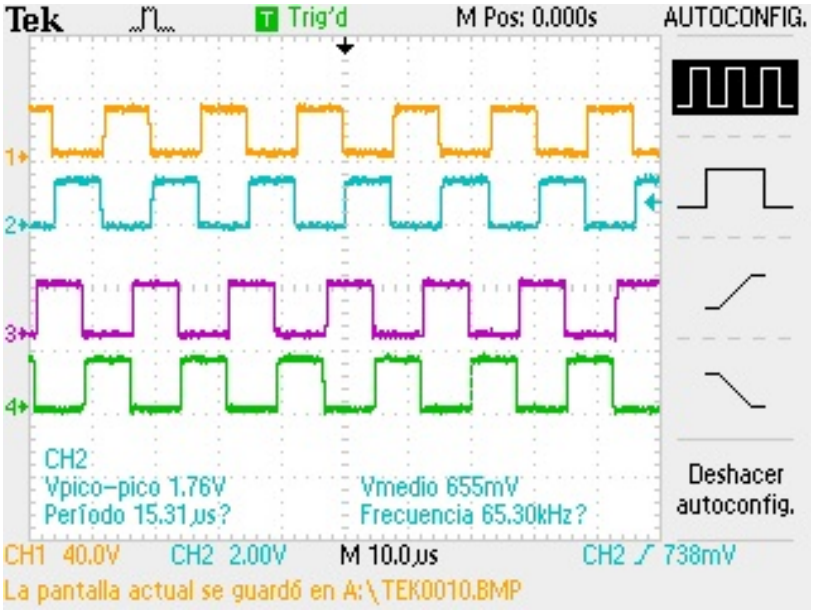

Figure 5-2: Switching Signals, out of the drivers at the frequency of 65.30kHz

5.3 PRC Results

After adequately firing the power switches, the output voltage will be looking similar to the one in the figure (4-2). Due to the control circuit design, we have the arbitrarity to choose the frequency and the duty. We choose the switching frequency purposely to send much current needed on the load, as the PRC at the end will be working as current source. Here it is considered that our load is fixed in value, due, the increase in switching frequency implies increase in current transfered to the load, therefore the increase in the ouptut voltage and power transfer in some cases. But, even if we switch at higher frequency to have the voltage required at the load; we have to make sure that we keep switching at a frequency greater than resonance value, to avoid switching losses. For the PRC above resonance frequency, it has an inductive behavior, therefore we will experience soft-switching during turn on and hard switching during turn-off of the power switches. We keep this behavior due to the fact that the solution can be got to remede the losses in case. In that way, with another arbitrarity given by the control circuit, we can continue to change the duty, to make sure that we keep the soft-switching at turn-on and hard-switching at turn-off. Following different modes of operation discussed before, it can be said that we are working in mode II, considering

the results in figure.(5-3). Due, we don't transfer power to the load, it is like power oscillation, as it cancel itself during the oscillations. The figure 5-3 was recorded also

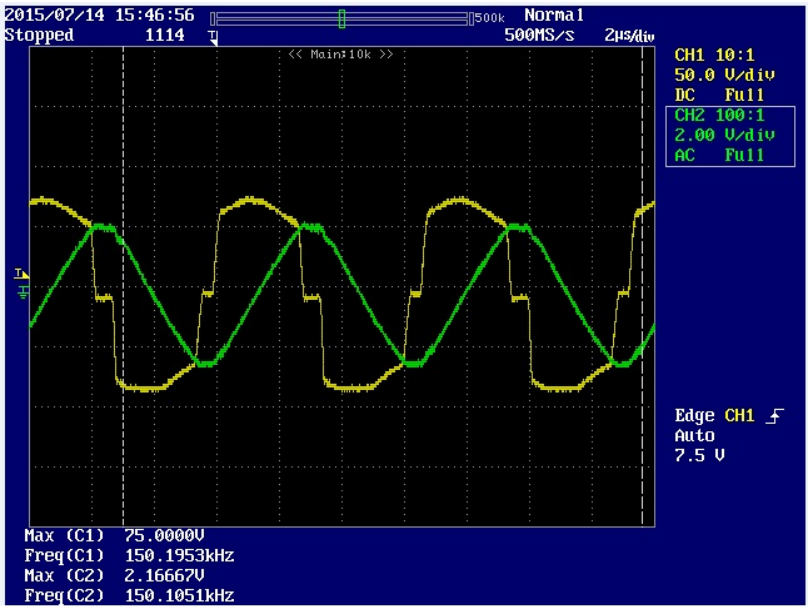

Figure 5-3: PRC voltage and current at a switching frequency of 150.1kHz

when the supply DC voltage was $35V_{dc}$, at the switching frequency of $150.1kHz$, the output DC voltage was $389.92V_{dc}$. This shows the very big gain we can experience; when comparing the input voltage to output voltage, the gain will be around 11.14. It is a very huge gain, and gives a hope to connect our HVDC E-beam to a low voltage DC source.

5.4 Measuring Circuit Results

As illustrated in figure. 4-7, the voltage V_{in}, will be the output voltage of the PRC system, and the V_out will be the needed voltage at the scale of 10000 : 1, the V_out will be supplied to the Vc terminal of the Figure (4-11). It was shown previously that the voltage at pin 7 of the **XR-2206** IC, must be lesser than $3V_{DC}$, in order to have frequency at Pin 11 of the same IC. So the chosen measuring scale is big enough, so that the maximum voltage that can be measured is $30kV_{DC}$. Due will be having frequency at any value of the measured voltage below $30kV_{DC}$. Here it

can be reminded that the voltage measured is converted into frequency following the Equation.4.6; that was made following the results displayed in the table. A.1. For matter of safety and security as it was also noted previously; the small voltage was used for retrieving sample results, the scale for the voltage divider circuit shown in figure. 4-7, was changed to $10:1$, and the maximum measured voltage was $30V_{DC}$. It can be seen that at the scale of the results more or less match our expectation.

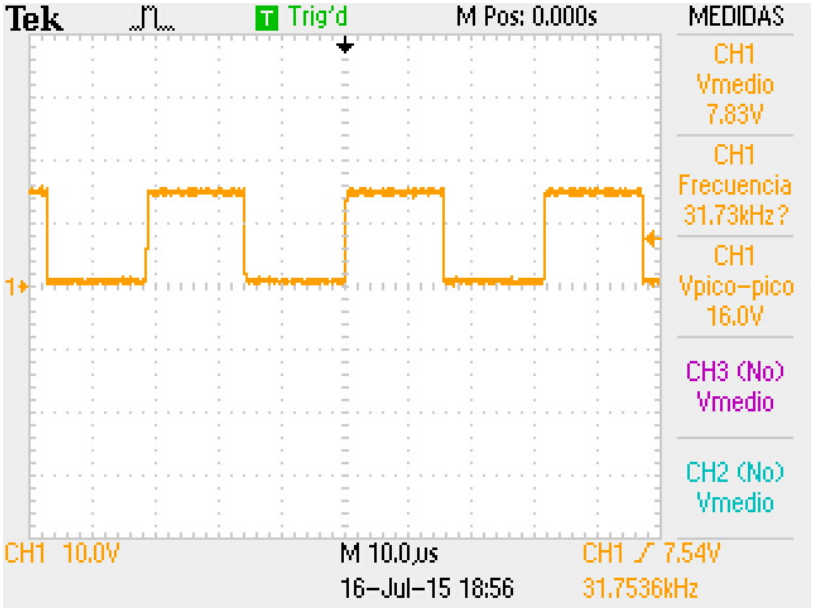

Figure 5-4: Measured signal at the voltage of $24.45V_{dc}$, the signal frequency was of $31.7536kHz$, respecting the equation. 4.6

The signal shown in figure.5-4, was the one transmitted over the fiber optic media, and will be having a shape as in the figure. 5-5. In the figure 5-5, the signal does not exactly achieve zero value, this is due to the diode voltage of $0.7V_{dc}$, the character of the diode in the fiber optic transmitter.

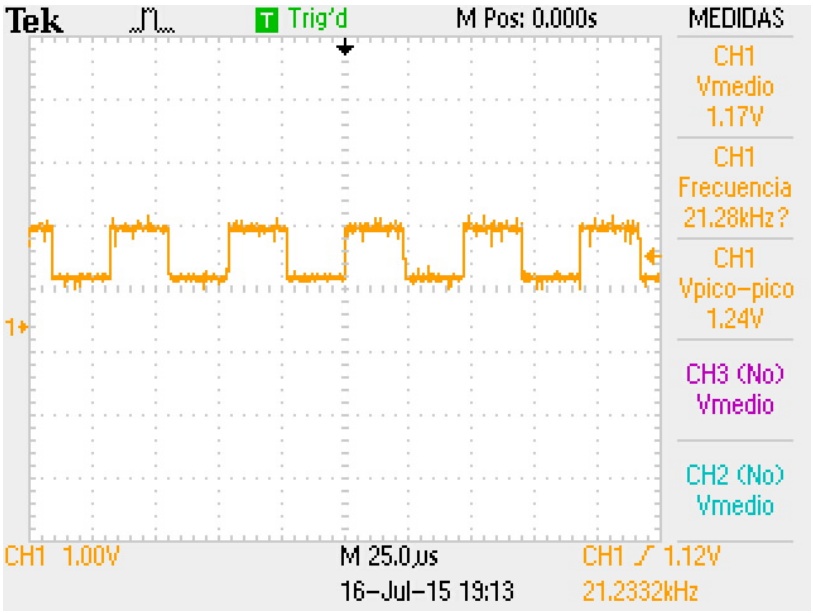

Figure 5-5: The signal transmitter over the fiber optics media corresponding to $27.4V_{dc}$

.

Chapter 6

Conclusions

In conclusion, it was seen from the early beginning of the project that following the development of electronics, Power electronic and computer, the industrial area has experienced a significant change in energy conversion. Where energy usage can be managed following the will of the user. Due, the high voltage device can be used connected to the lower voltage sources. From the beginning we considered the example of the E-beam welding machine. The last was detailed in its review literature. And was shown in figure.(2-1) and figure. (2-2); to clarify there working principle. After seing that it requires to work at high voltage DC; the parallel resonant converter was proposed. As it is shown in figure.(3-2), the full brigde converter was built using power MOSFET and switched by the firing signals generated by the control circuit at a frequency between $100kHz$ to $200kHz$, strengthened by the driver circuits and the arbitrarity to choose the duty as we need. For the purpose of having the signal shown in figure.(5-3). The Parallel Resonant Converter here played major role in order to have a required shape of current and voltage and adequately transferring power to the load, due the definition of different modes of operation discussed. Even if the required voltage was to achieve $3.5kV_{DC}$, for security issues we supplied a smaller voltage due the output voltage was at the maximum $389.92V_{dc}$ while the input DC voltage was only $35V_{dc}$, a gain of 11.14 was experienced; which was the proof to achieve the targeted value once the input supply voltage is increased. For different purposes we need to monitor the value of the output voltage, which was the main target of this

project. To design a HVDC measuring circuit. The measuring circuit was designed based on voltage divider principal as illustrated in the figure.(4-7); with the voltage scale of 10000 : 1; as the measuring circuit at this point share the same ground with the power circuit; the isolation is required for user protection. Different isolating methods were discussed but finally the fiber optic was considered. Due to the fact that the fiber optic transmitter and receiver available to our lab accept only digital signals; it was required to transform the change in measured voltage in frequency, using the IC illustrated in figure.4-10. The maximum measured voltage expected is $30kV_{DC}$, and will be corresponding to the minimum frequency we will have following the equation.4.6; generated following the results displayed in the table.A.1. In other words, the work was completed by having the possibility to generate a HVDC for our E-beam welding machine, and we have been successfully able to monitor the output voltage.

Chapter 7

Future Work

In this work, for safety issues, the system was not tested at that high expected voltage. For next work, it is recommended to have deepened study on high voltage required insulations for the purpose of having this test at a required values without problem. The frequency and duty values for switching the full bridge converter power switches; are changed manually; another study can be made to make an automatic control of both these control parameters. The measured value of the output voltage is converted to frequency; but it was not brought back to voltage and display the exact value. The next work should include the micro-controller programmed with all of those scales and equations; so that it will be processing the measured value and display the exact measured value on the screen for user purposes. A deep study will be made for the future to be able to make the design suitable to measure voltage more than $30kV_{DC}$, this will be achieved by continuing to try the possibility of using **Voltage Divider** method as well as other possibilities and methods like: Measuring High- Voltage DC based on Pockels Effect, based on DC Electric Field and DC field Probe. Other work also can be carried out to measure the current both primary and secondary sides of the transformer. Thinking also different ways to make the voltage-frequency interface circuit more accurate in higher and lower values of measured voltage.

Appendix A

Tables

Table A.1: Voltage -Frequency relationship of the voltage measured value.

Voltage[V]	Frequency [kHz]
0.4	91.5
0.5	89.5
0.6	86.8
0.7	84.5
0.8	82.0
0.9	78.0
1.0	75
1.1	72.7
1.2	69.5
1.3	66.2
1.4	63.7
1.5	60.6
1.6	58.5
1.7	55.0
1.8	51.8
1.9	48.2
2.0	44.0
2.1	42.3
2.2	37.7
2.3	34.8
2.4	31.7
2.5	29.6
2.6	26.4
2.7	21.4
2.8	19.41
2.9	16.1
3.0	12.2

Table A.2: Voltage -Decade voltage ratios using Standard Values[3].

Target voltage ratio	R2/R1	R1 (E24/96)	R2 (E12)	Actual Voltage Ratio	Nominal Error
10:1	9	9K1	82K	10.01	0.1%
100:1	99	4K75	470K	99.95	-0.05%
1000:1	999	1K0	1M0	1001	+0.1%
1000:1	999	6K81	6M8	999.5	-0.05%
10000:1	9999	1K0	10M	10001	0.01%

Table A.3: Clock Frequency and related capacitance[2].

Frequency Range[kHz]	Capacitance [F]
$f_{clock} < 30$	2.2n
$30 < f_{clock} < 100$	680p
$100 < f_{clocck}$	220p

Appendix B

Figures

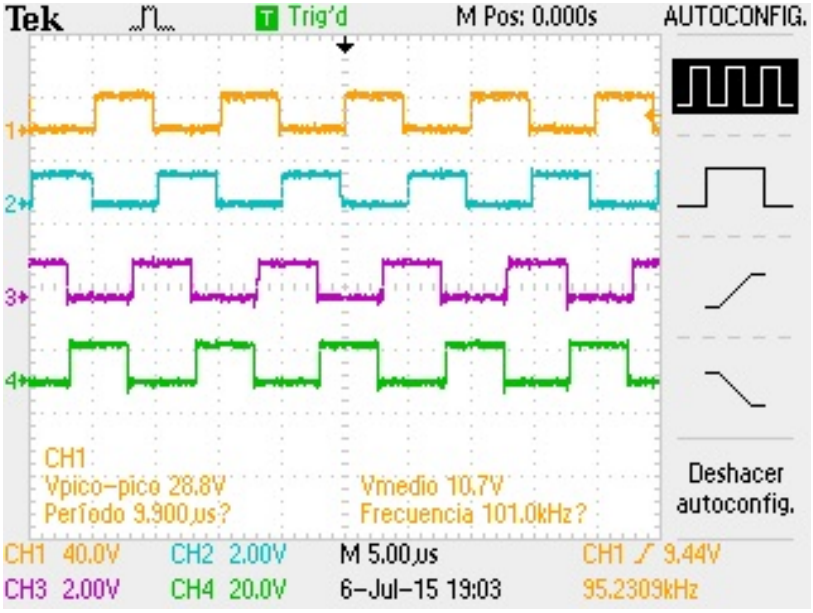

Figure B-1: Control circuit output Signals at the frequency of 101kHz.

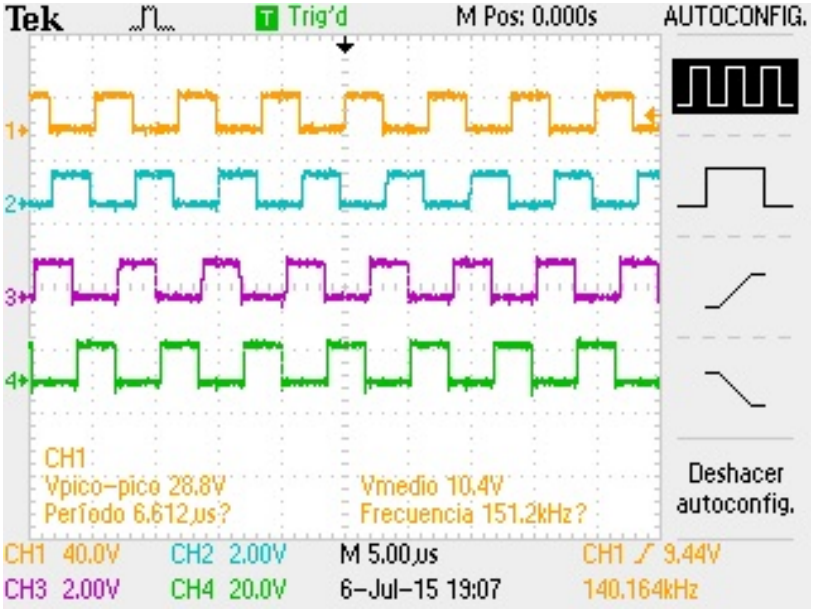

Figure B-2: Control circuit output Signals at the frequency of 151.2 kHz.

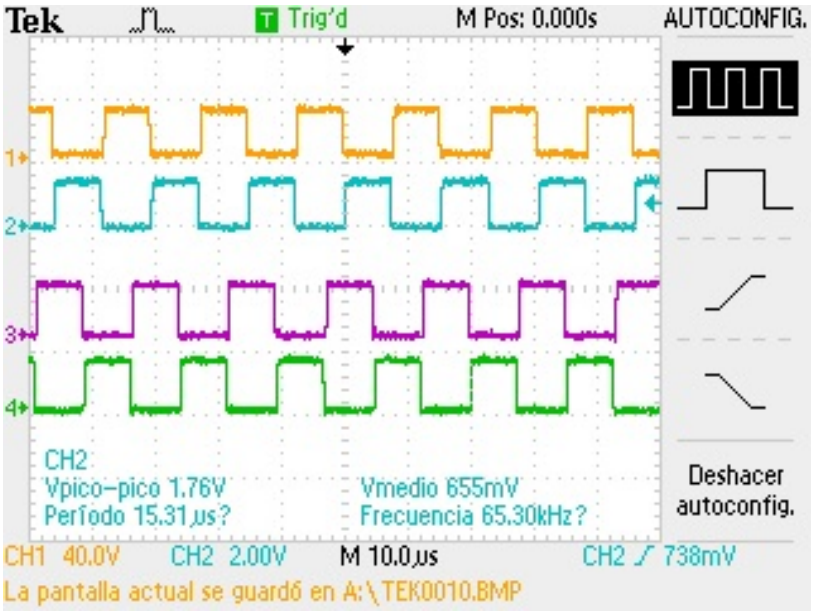

Figure B-3: Driver circuit output Signals at the frequency of 65.30 kHz.

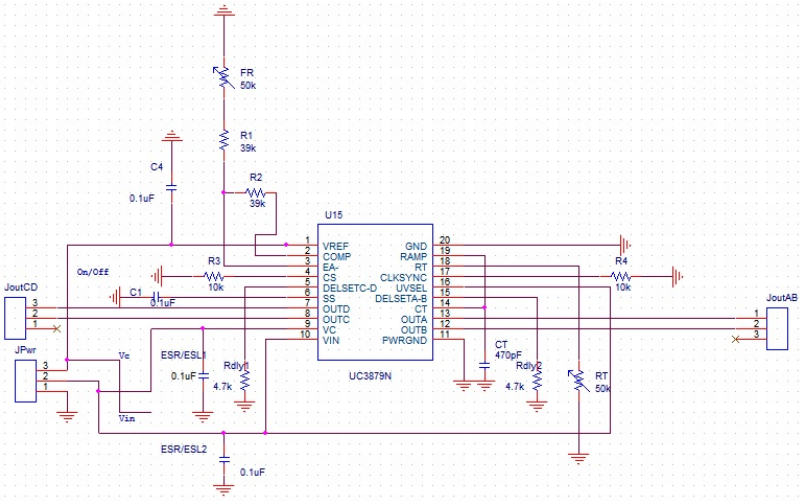

Figure B-4: Control circuit model

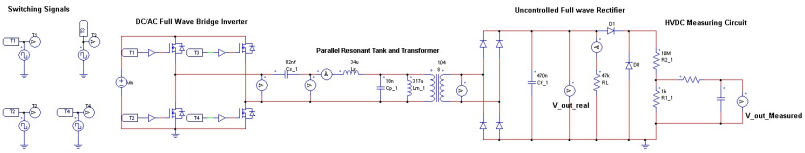

Figure B-5: The full model as simulated in Psim, the E-Beam Machine here is represented by a Load Resistance R_L.

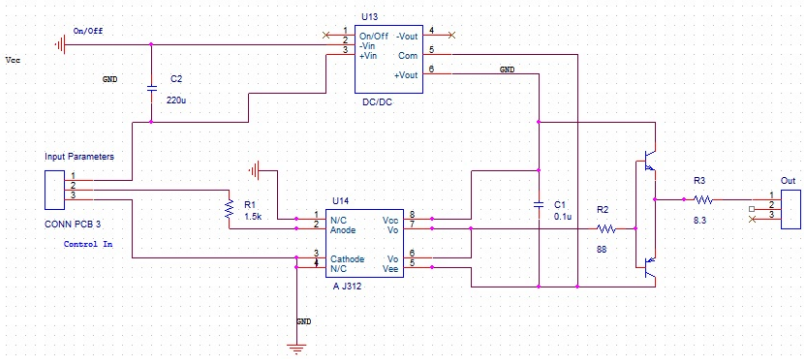

Figure B-6: Driver Model.

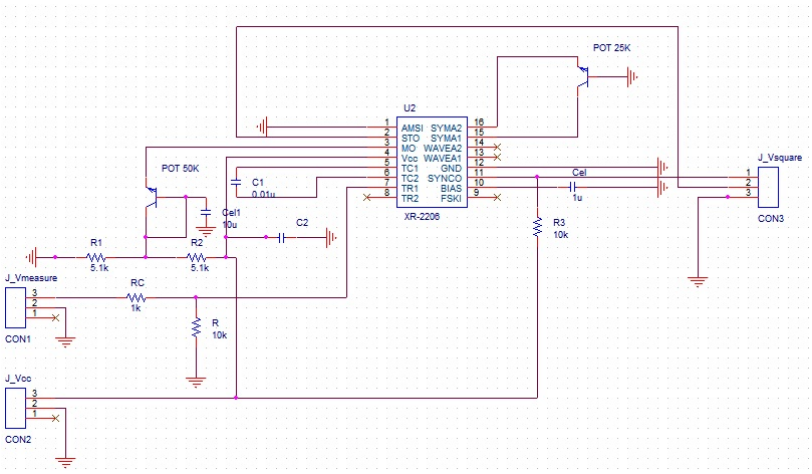

Figure B-7: Voltage to frequency Interface model built in Cadence, POT stands for potentiometers, the transistors were only used to model a three terminal potentiometer at in the library, the only available is two terminals.

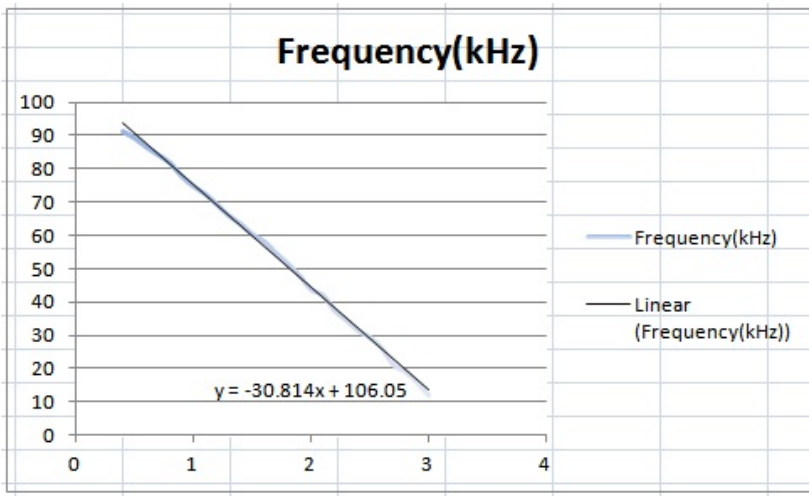

Figure B-8: Voltage-Frequency equation illustration as shown in table A.1.

Bibliography

[1] XR EXAR....the analog plus company^{TM}. $XR-2206 Monolithic Function Generator$, 2008.

[2] Laszlo Balogh. *THE NEW UC3879 PHASE-SHIFTED PWM CONTROLLER SIMPLIFIES THE DESIGN OF OF ZERO TRANSITION FULL-BRIDGE CONVERTERS*, 1999.

[3] TT Electronics. *Fixed Resistors, RESISTORS FOR HIGH VOLTAGE APPLICATIONS, Application Note.*

[4] IEEE; Pedro Jose Villegas Saiz Member IEEE; Juan A. Martin-Ramos Member IEEE; Alberto MArtin-Pernia Member IEEE Juan Diaz, Member and IEEE. Juan A. Martinez, Member. A high-voltage ac/dc resonant converter based on prc with single capacitor as an output filter. *IEEE TRANSACTIONS ON INDUSTRY APPLICATIONS Journal*, 46(6), 2010.

[5] Robert W. Erickson; Dragan Maksimovic. *Fundamentals of Power Electronics*, chapter 5.19. Kluwe Academic Publishers, 2004.

[6] ME. Electron beam machining (ebm) - modern machining process. *http://www.me-mechanicalengineering.com/2014/11/electron-beam-machining.html*, 2014.

[7] AVGO Technologies. *HCPL-3120/J312,HCNW3120 2.5 Amp Output Current IGBT Gate Driver Opto-coupler Data Sheet*, 2013.

[8] AVGO Technologies. *HFBR-0500Z Series Versatile Link, The Versatile Fiber Optic Connection Data Sheet*, 2014.

[9] JOINING TECHNOLOGIES. Electron beam welding. *http://www.joiningtech.com/industry-references/welding-types/electron-beam-welding*, 2015.

[10] Wikipedia. Power supply and control and monitoring electronics. *http://en.wikipedia.org/wiki/Electron$_b$eam$_w$elding*, 2012.

[11] Wikipedia. Optical fiber. https://en.wikipedia.org/wiki/Optical$_f$iber, 2015.